

Cite this: *New J. Chem.*, 2011, **35**, 1054–1059

www.rsc.org/njc

PAPER

Fluorescence enhancement of a tetrazole-based pyridine coordination polymer hydrogel†

Ji Ha Lee,^a Hyejin Lee,^a Sungmin Seo,^a Justyn Jaworski,^a Moo Lyong Seo,^a Sunwoo Kang,^b Jin Yong Lee^{*b} and Jong Hwa Jung^{*a}

Received (in Montpellier, France) 28th October 2010, Accepted 24th February 2011

DOI: 10.1039/c0nj00840k

Hydrogelation of a pyridine derivative (**1**) possessing tetrazole moieties as end groups, without long alkyl chain groups, results in the formation of a Mg(NO₃)₂ coordination polymer gel. The polymer exhibits a strong fluorescence enhancement upon gel formation. **1** can also be gelled with a variety of magnesium anions such as SO₄²⁻, NO₃⁻, Cl⁻, Br⁻ and I⁻, indicating that the coordination polymer gel formation of **1** does not strongly depend on anions. The SEM and AFM images of Mg²⁺ coordination polymer gel **1** display a fibrillar network several micrometres long, with widths in the range of 60–70 nm and thicknesses of about 3 nm. In addition, photophysical studies show that the hydrogel exhibits a typical π–π* transition and gives rise to high fluorescence behavior. The coordination polymer hydrogel exhibits viscoelastic behavior as evidenced from the rheological studies.

Introduction

The self-assembly of small molecules to form functional materials is a powerful tool for the development of new device technologies. In particular, supramolecular self-assembly of low-molecular-mass organic gelators leading to gel formation has attracted increasing interest.^{1–17} Supramolecular gels have been studied as soft materials for use in applications such as drug-delivery systems, tissue engineering, sensing devices, separation and optoelectronic devices.^{1–17} Many researchers have successfully incorporated metal ions into organic gelators to form metallogels and coordination polymer gels.^{18–20} Metallogels and coordination polymer gels have been reported to show unusual functional properties such as redox responsiveness,^{21,22} catalytic action,^{23,24} absorption,^{25,26} emission,^{27–29} magnetism²⁶ and electron emission.²⁴ It has also been shown that the gelation of coordination polymers makes the material more processable for direct device applications.³⁰

To date, there is relatively little information in the literature regarding the photoluminescence properties of coordination polymer gels, including switching of the emission colour, field emission and light emitting properties.^{27–29} In view of the high photoluminescence quantum efficiencies of pyridine

derivatives used as fluorescent dyes,³¹ it is expected that such compounds may exhibit interesting spectroscopic and luminescence properties during the sol–gel transition reaction. In particular, fluorescent Mg²⁺ coordination polymeric gels are very rare²⁸ in comparison to transition metal ion gels.^{8,16,17,23,24,26} In addition, Mg²⁺ can take place in various coordination numbers. With this in mind, herein, we report the formation of a coordination polymer gel of tetrazole-appended pyridine derivatives (**1**) containing a Mg²⁺ ion, without long alkyl chain groups. In addition, we prepared ligand **2** without a central nitrogen atom as a reference. Remarkably, the fluorescence intensity is enhanced upon the formation of a coordination polymer gel, relative to **1** in aqueous solution. Of the few reports on the enhancement of photoluminescence intensity upon gelation, most utilize organic gels,³² two component gels³³ or emissive materials immobilized in a gel network.³⁴

Results and discussion

When a basic aqueous solution comprising ligand **1** or **2** is reacted with Mg²⁺ ions in solution, both **1** and **2** will form hydrogels instantly at pH = 12, as confirmed by the inverted test tube method (Fig. 1A, Fig. S1, ESI†, and Scheme 1). In addition, **1** forms hydrogels with Cu²⁺, Co²⁺, Zn²⁺ and Ni²⁺ ions at pH = 12 (Fig. S2, ESI†). No gelation was observed when the same reaction was repeated with other solvents. Hydrogel **1** is pH responsive and precipitates upon adjustment to acidic pH values. On adjusting the pH to a strong basic condition (pH = 12–14), the formation of a complex allows the recovery of the gel structure. **1** can also be gelled with a variety of magnesium anions such as SO₄²⁻, NO₃⁻, Cl⁻, Br⁻

^a Department of Chemistry and Research Institute of Natural Science, Gyeongsang National University, Jinju 660-701, Korea.
E-mail: jonghwa@gnu.ac.kr

^b Department of Chemistry and Institute of Basic Science Sungkyunkwan University, Suwon 440-746, Korea.
E-mail: jinylee@skks.edu

† Electronic supplementary information (ESI) available: Details of experimental section, SEM and TEM images, pictures of coordination polymer gel **1** and spectroscopic data. See DOI: 10.1039/c0nj00840k

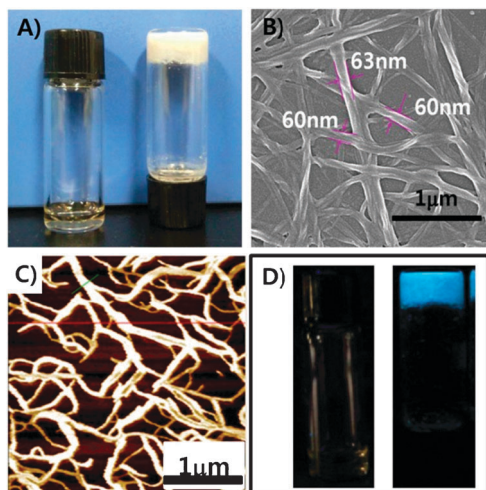
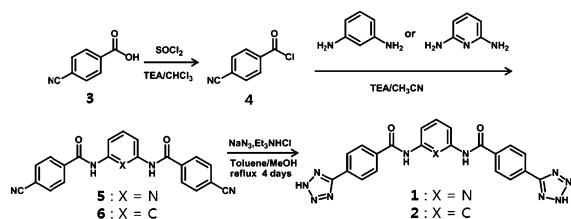


Fig. 1 (A) Photograph of sol **1** (left) and gel **1** (20 mM, right) with Mg^{2+} (80 mM, 4 equiv.). (B) SEM and (C) AFM images of gel **1**. (D) Photograph of sol **1** (left) and gel **1** (20 mM, right) with Mg^{2+} (80 mM, 4 equiv.) by irradiation with UV light.



Scheme 1 Synthetic route of ligands **1** and **2**.

and I^- (Fig. S3, ESI[†]), indicating that the coordination polymer gel formation of **1** does not strongly depend on anions.

Fig. 1B and C show the SEM and AFM images of Mg^{2+} coordination polymer gel **1**, which clearly display a fibrillar network. The fibers are several micrometres long with widths in the range of 60–70 nm and thicknesses of about 3 nm. SEM images of Mg^{2+} coordination polymer gel **1** with different anions showed a similar fiber structure with diameters of 50–100 nm (Fig. S4, ESI[†]). These findings suggest that the morphology of the coordination polymer gel **1** did not strongly depend on the nature of the anion.

We attempted to determine the crystal structures of the related complexes to understand the coordination behaviors between ligand **1** and Mg^{2+} , but repeated efforts were not successful. As an alternative, we obtained the X-ray powder diffraction pattern of freeze dried Mg^{2+} coordination polymer gel **1**. The tetrazole groups serve as multi-binding sites to form a 2D or 3D coordination polymer in the presence of an excess of metal ions.^{35,36} As shown in Fig. S5, ESI[†], the X-ray powder diffraction pattern of Mg^{2+} coordination polymer gel **1** shows a crystalline nature. The Mg^{2+} coordination polymer gel **1** may correspond to an ordered 2D coordination polymer network structure.

To understand the coordinated molecular structure for **1** complexed with Mg^{2+} , we carried out density functional theory (DFT) calculations using Becke's three parameterized

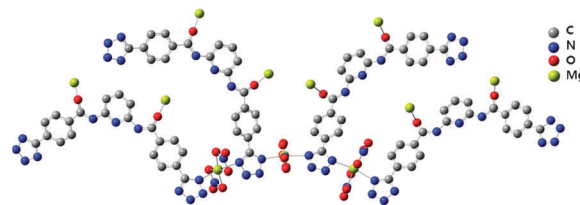


Fig. 2 The B3LYP/3-21G* optimized structure for **1** complexed with Mg^{2+} .

Lee–Yang–Parr exchange functional (B3LYP) employing 3-21G* basis sets using a suite of Gaussian 03 programs.³⁷ The optimized structure for **1**– Mg^{2+} complex is shown in Fig. 2. The two ligand **1** and two nitrate anions octahedrally coordinated to Mg^{2+} cation with *trans* conformation, where the nitrate anions function as bidentate ligands. The distances between the nitrogen of **1** and Mg^{2+} were calculated to be in the range of 2.19–2.36 Å, while the distances between the oxygen atoms of nitrate and Mg^{2+} were in the range of 2.02–2.06 Å. Using the above optimized structure, we generated an expanded 2D framework through the proper interactions and coordination as shown in Fig. S6, ESI.[†] In ligand **1**, only two nitrogen atoms can coordinate to Mg^{2+} ion. In contrast, the other two nitrogen atoms of the tetrazole unit of **1** did not bind to Mg^{2+} , due to a steric hindrance effect. This result is in agreement with previous results reported by Prof. J. R. Long. In addition, as seen in the calculated structures, each tetrazole ligand **1** can bind to 6 Mg^{2+} ions, of which 4 Mg^{2+} can be shared with another tetrazole ligand. In addition, the oxygen atoms of the amide groups of the tetrazole ligand **1** can be coordinated to 2 Mg^{2+} ions. Thus, stoichiometrically each tetrazole ligand can bind to 4 Mg^{2+} ions on average, which is consistent with experiment.

The absorption and emission properties of sol **1** and coordination polymer gel **1** with metal ions were extensively studied. The UV-vis absorption band of Mg^{2+} coordination polymer gel **1** appears at 302 nm (Fig. 3A), a typical π – π^* transition.^{12,13} On the other hand, the π – π^* absorption band of sol **1** exhibits a 70 nm blue shift. The fluorescence spectra of the coordination polymer gel **1** ($\lambda_{\text{exc}} = 302$ nm) were also obtained. As shown in Fig. 3B, Mg^{2+} coordination polymer gel **1** exhibits a strong blue emission with a maximum at $\lambda = 467$ nm. The fluorescence intensity is enhanced drastically

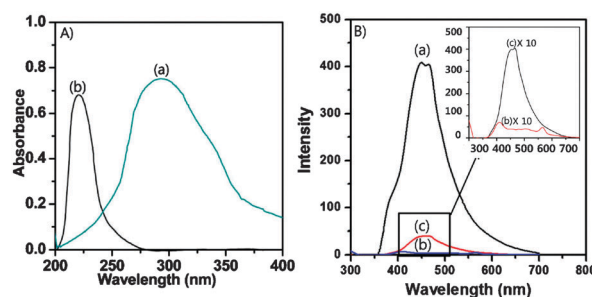


Fig. 3 (A) UV-vis spectra of (a) gel **1** (20 mM) with Mg^{2+} (80 mM, 4 equiv.) and (b) sol **1** (20 mM) without Mg^{2+} . (B) Fluorescence spectra of (a) gel **1** (20 mM, $\lambda_{\text{exc}} = 302$ nm) with Mg^{2+} (80 mM, 4 equiv.), (b) sol **1** (20 mM, $\lambda_{\text{exc}} = 220$ nm) without Mg^{2+} and (c) solid **1** (20 mM) with Mg^{2+} (80 mM, 4 equiv.) obtained at pH = 3.

compared to sol **1**. On the other hand, the fluorescence intensity of the precipitated solid **1**–Mg²⁺ obtained at pH = 3 is much weaker than that of Mg²⁺ coordination polymeric gel **1** (Fig. 3B(c)), because the solid **1** complexed with Mg²⁺ might form H-type aggregation due to strong π – π stacking.³⁸ The photoluminescence of Mg²⁺ coordination polymer gel **1** can be seen by the naked eye under UV light (Fig. 1D). The planar conformation of **1** may be induced in the gel state due to the strong intermolecular forces, which tend to optimize close packing between molecules. This aggregation-induced planarization extends the effective aromatic groups in ligand **1** molecule. Furthermore, in the gel state, the coordination polymer structure of **1** with Mg²⁺ plays an important role of favoring J-type aggregation, which restricts the formation of the excimer complex.³⁹ Consequently, molecule **1** in the aggregated gel state is likely to show drastically enhanced fluorescence emission compared to that of the isolated state due to the synergetic effect of intramolecular planarization and restricted excimer formation. In contrast, the fluorescence emission intensity of the Co²⁺, Zn²⁺, Ni²⁺ and Cu²⁺ coordination polymeric gel **1** decreased drastically compared to Mg²⁺ coordination polymer gel **1**, due to the photoinduced electron transfer (PET) effect, which occurred upon complex formation between the nitrogen atoms of both end tetrazole groups of ligand **1** and Co²⁺, Zn²⁺, Ni²⁺ and Cu²⁺ (Fig. S7, ESI†).⁴⁰

Interestingly, the fluorescence intensity of Mg²⁺ coordination polymer gel **1** gradually increased until the addition of 4 equivalents of metal ion and remained constant upon further addition (Fig. S8, ESI†). These results indicate that one molecule of gelator **1** binds to 4 metal ions. Furthermore, we observed the fluorescence properties of Mg²⁺ coordination polymer gel **1** with different anions such as Cl[–], Br[–], I[–] and SO₄^{2–}. To probe the stoichiometry, we prepared the precipitation of **1** upon the addition of an excess of Mg²⁺ (6.0 equivalents) at pH = 3. To remove the uncoordinated Mg²⁺, the solid product was washed with aqueous solution. The solid sample, containing ligand **1** and Mg(NO₃)₂, was examined by elemental analysis and ICP analysis. Elemental analysis and ICP of the precipitated sample demonstrated a content profile of 23.99% for C, 1.43% for H, 25.37% for N and 9.32% for Mg. Our DFT calculations also show the following results, which are in excellent agreement with the experimental data: calculated C(24.09%), H(1.44%), O(39.74%), N(25.42%), Mg(9.29%). These findings indicate that the stoichiometry of sample is consistent with a 4 : 1 formulation. The Mg²⁺ coordination polymer gel **1** with NO₃[–] exhibits the strongest emission. In contrast, a quenching effect was observed for gel **1** with MgBr₂ and MgI₂, induced by this intersystem crossing.⁴¹ In particular, the binding strengths for Br[–] and I[–] coordinated to Mg²⁺ might be stronger than that of NO₃[–], thereby inducing a large quenching effect.

Controlled experiments were conducted to investigate whether the fluorescence enhancement arises from the coordination polymer gel formation or from complexation with Mg²⁺. The emission properties of the solution of **1** (20 mM) upon addition of Mn²⁺ (4 equiv.) were studied. Even though **1** might form a simple complex with Mn²⁺ in aqueous solution, the solution **1** with Mn²⁺ demonstrates non-emission. There were

two possibilities for non-emission of **1** with Mn²⁺. The first is due to the photoinduced electron transfer (PET) effect, which occurred upon complex formation between the nitrogen atoms of both end tetrazole groups of ligand **1** and Mn²⁺. The second is related to the complex structure between **1** and Mn²⁺. In this study, the non-emission of **1** with Mn²⁺ is primarily related to the complex structure. This finding indicates that the strong fluorescence observed for gel **1** with Mg²⁺ originates from the coordination polymer structure.

Fluorescence of the coordination polymer gel **1** was also measured as a function of temperature, as shown in Fig. S10, ESI†. No significant spectral changes were observed until 55 °C. The fluorescence intensity of Mg²⁺ coordination polymer gel **1** with NO₃[–] slightly decreases at 57 °C. Further increase in temperature resulted in a large reduced emission. These results suggest that the emission of the coordination polymer gel **1** decreases as it starts to melt at 55–59 °C. The decreasing fluorescent intensity of gel **1** above 56 °C is due to this transformation to a solution phase. This phenomenon is the same to that observed with Mn²⁺.

The optimal emission of **1** therefore occurs when the gel is completely formed and decreases as the gel melts at higher temperature. This striking observation may be attributed to the rigidification of the media upon gelation, a process that slows down nonradiative decay mechanisms, leading to luminescence enhancement. Though the gel dissociates from the aggregated state and shows a drastic drop in fluorescence intensity, the complex still exhibits a considerable blue emission in the solution state. This may be due to weak supra-molecular interactions while still in the solution state.

To garner an insight into the thermally promoted stability of Mg²⁺ coordination polymer gel **1**, the transition temperature ($T_{\text{sol-gel}}$) of coordination polymer gel **1** was measured by differential scanning calorimetry (DSC) (Fig. S11, ESI†). Mg²⁺ coordination polymer gel **1** showed a sharp phase transition at 56 °C, an endothermic reaction. This endothermic thermogram is due to the transition of the Mg²⁺ coordination polymer gel **1** into a solution phase as observed in Fig. S10, ESI†. This sol–gel transition temperature of Mg²⁺ coordination polymer gel **1** is consistent with the results obtained by fluorescence spectroscopy.

The luminescence properties of Mg²⁺ coordination polymer gel **1** were studied by time-resolved fluorescence confocal microscopy. The emission decay profiles were monitored at $\lambda = 405$ – 490 nm for Mg²⁺ coordination polymer gel **1** (Fig. 4). The fluorescence decay of Mg²⁺ coordination polymer gel **1** was fitted with a single exponential component yielding a

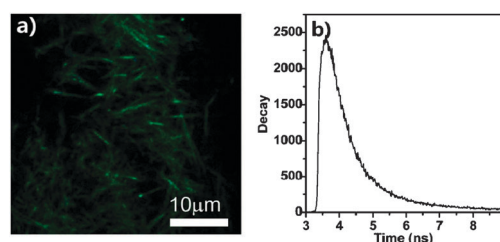


Fig. 4 (a) Fluorescence image of Mg²⁺ coordination polymer gel **1** by time-resolved fluorescence confocal microscopy and (b) its fluorescence decay.

lifetime of 3.78 ns, indicating that this emission is fluorescence. This result reflects the fact that coordination polymer gel **1** in its aggregated state is more rigid, restricting the rotational and vibrational movements of molecules. In contrast, the fluorescence lifetime of solid **1** was less than 2.3 ns (Fig. S12, ESI†). The limited molecular motions decrease the nonradiative relaxation process, which leads to the longer lifetime and fluorescence enhancement.⁴²

To understand the mechanical properties of hydrogel **1**, dynamic oscillation and steady shear measurements were carried out. The linear viscoelastic region (LVR) of Mg²⁺ coordination polymer gel **1**, as a function of the amplitude of deformation on shear, was determined with a strain amplitude ranging from 0.01% to 100% at 1 rad s⁻¹ (Fig. S13A, ESI†). Both the in-phase storage modulus (G') and the out-of-phase loss modulus (G'') remain constant up to ~1% strain ($G' > G''$), an outcome which defines the uppermost bound of LVR. Beyond this level of deformation, a catastrophic disruption of the network occurs as indicated by the steep drop in the values of both moduli and the reversal of the viscoelastic signal ($G'' > G'$). Based on these data, we decided to perform subsequent measurements on the gel at 0.1% strain, which lies comfortably within LVR.

Time-dependent oscillation measurements were used to monitor the gelation process of Mg²⁺ coordination polymer gel **1**, which forms gradually upon mixing of ligand **1** and Mg²⁺ (Fig. S13B, ESI†). The time sweep shows the rapid growth of G' and G'' in the initial stage of gelation followed by a slower long term approach to a final pseudo-equilibrium plateau. At the end of the experiment, the value of G' was about an order of magnitude higher than G'' . Gel network formation as evidenced by the time dependent oscillation is consistent with the fluorescence studies, which showed that the maximum fluorescence intensity is reached at about 2 min.

Once the aforementioned pseudo-equilibrium plateau was reached, we were able to implement a frequency sweep between 0.1 and 100 rad s⁻¹ at the same temperature and within the LVR (Fig. 5A). The results show that $G' > G''$, confirming that the Mg²⁺ coordination polymer **1** has predominantly an elastic character. The elasticity of the gel is further evident from the fact that G' and G'' are minimally sensitive to ω and the loss tangent ($\tan \delta = G''/G'$) approaches a value of ~0.1 in the tested frequency range. The double logarithmic plot of η^* (dynamic viscosity) versus (angular frequency) shows a gradient close to -1 [note: $\eta^* = (G'^2 + G''^2)^{1/2}/\omega$],

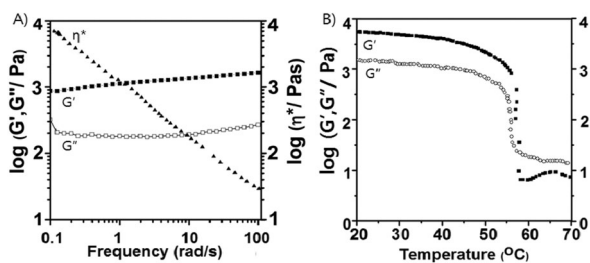


Fig. 5 (A) Frequency sweep of G' and G'' for Mg²⁺ coordination polymer gel **1** at a strain of 0.1%. (B) Temperature ramp G' and G'' for Mg²⁺ coordination polymer gel **1** at the heating rate of 1 °C min⁻¹, strain of 0.1% and frequency of 1 rad s⁻¹.

which is a characteristic of a strong cohesive gel.⁴³ A sharp melting process then ensues, which results in “liquefaction” of the sample between 54–57 °C, indicating a thermally labile assembly (Fig. 5B). This observation is consistent with the variable temperature fluorescence studies.

Conclusions

In conclusion, we have demonstrated that the formation of a coordination polymer gel can be facilitated without long alkyl chain groups. A tetrazole-appended ligand is shown to efficiently produce a hydrogel by simple mixing with Mg²⁺. Photo-physical studies show that the hydrogel exhibits a typical π - π^* transition and gives rise to high fluorescence behavior. Upon the formation of the coordination polymer gel, the complex shows a pronounced fluorescence enhancement with a long lifetime, as compared to the ligand. Together, measurements of dynamic oscillation and steady shear indicate the formation of a weak and thermally labile network whose tenuous supramolecular structure is irreversibly disrupted by mechanical and thermal treatments.

Experimental

Equipments

¹H and ¹³C NMR spectra were measured on a Bruker ARX 300 apparatus. IR spectra were obtained for KBr pellets, in the range 400–4000 cm⁻¹, with a Shimadzu FT-IR 8400S, and Mass spectra were obtained by a JEOL JMS-700 mass spectrometer. The optical absorption spectra of the samples were obtained at 378–278 K using a UV–vis spectrophotometer (Hitachi U-2900). All fluorescence spectra were recorded in a RF-5301PC spectrophotometer. The powder X-ray diffraction (XRD) measurements of the samples were recorded on a Bruker D8-Advance X-ray powder diffractometer using Cu K α radiation ($\lambda = 0.1542$ nm) with scattering angles (2θ) of 3–70°, operating at 40 keV, cathode current of 20 mA. Differential scanning calorimetry (DSC) was performed on a Seiko DSC6100 high-sensitivity differential scanning calorimeter equipped with a liquid nitrogen cooling unit. Samples of the self-assembled metal coordination polymeric gel were hermetically sealed in a silver pan and measured against a pan containing alumina as the reference. The thermograms were recorded at a heating rate of 1 °C min⁻¹. Scanning electron micrographs of the samples were taken with a field emission scanning electron microscope (FE-SEM, FEI Sirion 400). The accelerating voltage of SEM was 5–15 kV and the emission current was 10 μ A. Atomic force microscopy (AFM) images were taken on an AutoProbe CP/MT scanning probe microscope (XE-100(PSIA)). Imaging was done in non-contact mode using a V-shaped ‘Ultralever’ probe B (Park Scientific Instruments, boron doped Si with frequency $f_c = 78.6$ kHz, spring constants $k = 2.0$ – 3.8 N m⁻¹, and nominal tip radius 10 nm). All images were collected under ambient conditions at 50% relative humidity and 23 °C with a scanning raster rate of 1 Hz. Samples for AFM images were prepared by depositing dispersions of hydrogel **1** in EtOH on a freshly cleaved mica surface (Ted Pella Inc. Prod No. 50) and allowing them to dry in air.

Rheological measurements

These were carried out on freshly prepared gels using a controlled stress rheometer (AR-1000N, TA Instruments Ltd, New Castle, DE, USA). Parallel plate geometry of 40 mm diameter and 1.5 mm gap was employed throughout. Following loading, the exposed edges of samples were covered with a silicone fluid from BDH(100 cs) to prevent water loss. Dynamic oscillatory work kept a frequency of 1.0 rad s⁻¹. The following tests were performed: increasing the amplitude of oscillation up to 100% apparent strain on shear, time and frequency sweeps at 25 °C (60 min and from 0.1–100 rad s⁻¹, respectively), and a heating run up to 90 °C at a scan rate of 1.0 °C min⁻¹. Unidirectional shear routines were performed at 258 °C covering a shear-rate regime between 10⁻¹ and 10³ s⁻¹. Mechanical spectroscopy routines were completed with transient measurements. In doing so, the desired stress was applied instantaneously to the sample and the angular displacement was monitored for 60 min (retardation curve). After completion of the run, the imposed stress was withdrawn and the extent of structure recovery was recorded for another 60 min (relaxation curve). Dynamic and steady shear measurements were conducted in triplicate and creep (transient) measurements in duplicate.

Fluorescence lifetime microscopy (FLM) measurements

Fluorescence lifetime images were acquired by an inverse time resolved fluorescence microscope, MicroTime-200 (PicoQuantGmBH). The excitation wavelength, the spatial resolution, and the time resolution were 405 nm, 0.3 μm, and 60–70 ps, respectively. The samples were prepared on one side of microscope cover glasses. The manufacturer's software was used to analyze the data and calculate the lifetime maps. The color scales represent average lifetime and total number of counts is indicated by color density at each point.

Preparation of the metal coordination polymer gel

In a vial, the solution of metal salt [0–4 equiv.] was added to solution of gelator (3–5 wt%). The metal coordination polymeric gel is formed immediately upon standing in ambient temperature. The resulting reaction mixture was subjected to sonication. The metal coordination polymeric gel was stable to inversion of the vial.

Compound 5

Thionyl chloride (5.9 g, 50 mmol) was added dropwise to compound **3** (7.4 g, 50 mmol) and triethylamine (5.1 g, 50 mmol) in chloroform. The mixture was refluxed for 2 h and cooled down to room temperature. Then an acetonitrile solution of 2,6-diaminopyridine (2.7 g, 25 mmol) and triethylamine (5.1 g, 50 mmol) were added dropwise to the resulting compound **3** solution, cooled by salt and ice water. The solution was stirred for 12 h, and then water was added. From the resulting solution, yellow powder was filtered and washed with a dilute Na₂CO₃ solution, distilled water, and then a small amount of cold methanol. Compound **5** was obtained as yellowish white powder (5.4 g, 59%). ¹H NMR (300 MHz, DMSO-d₆) 10.88 (s, 2H, NH), 8.13 (d, ²J(H,H) = 8.1 Hz, 4H; Ar-H), 8.02 (d, ²J(H,H) = 8.1 Hz, 4H; Ar-H), 7.899 (t, ³J(H,H) = 6.9 Hz, 3H; Ar-H). ¹³C NMR (DMSO-d₆)

δ = 164, 158, 139, 138, 132, 128, 119, 116, 99 ppm. IR (KBr, cm⁻¹): 3364, 3335, 3093, 3063, 2229, 1678, 1662, 1533, 1522, 1490, 1447, 1300, 1238, 1159, 1114, 1085, 1017, 990, 856, 830, 796, 754, 617, 575, 537. HRMS (FAB⁺) *m/z* 368.1069 [(M + H)⁺ calcd for C₂H₁₃N₅O₂: 368.1574]. Anal. calcd for C₂H₁₃N₅O₂: C, 68.71; H, 4.32; N, 19.43. Found: C, 68.66; H, 3.57; N, 19.06%.

Compound 1

A mixture of compound **5** (1 g, 27 mmol), NaN₃ (2.123 g, 330 mmol), and triethylamine hydrochloride (4.496 g, 330 mmol) in 100 mL of toluene and 10 mL of methanol was heated at reflux for 4 days. The precipitate was then collected by hot filtration and dissolved in aqueous NaOH (1 M). The resulting clear, colorless solution was titrated with HCl (1 M) until the pH of the solution was 4. The ensuing white precipitate was washed with successive aliquots of distilled water and diethyl ether to afford 0.5 g (41.7%) of the product. ¹H NMR (300 MHz, DMSO-d₆) 10.79 (s, 2H, NH), 8.30 (d, ²J(H,H) = 8.7 Hz, 4H; Ar-H), 8.20 (d, ²J(H,H) = 8.4 Hz, 4H; Ar-H), 7.92 (t, ³J(H,H) = 3.9 Hz, 3H; Ar-H). ¹³C NMR (DMSO-d₆) δ = 182, 165, 150, 140, 136, 129, 127, 112, 111 ppm. IR (KBr, cm⁻¹): 3486, 3314, 3093, 3053, 3025, 2922, 2858, 2830, 2759, 2720, 2696, 2668, 2633, 2587, 2521, 1979, 1644, 1588, 1524, 1495, 1455, 1311, 1287, 1237, 1124, 1089, 998, 904, 854, 797, 731, 710, 644, 632, 585, 532, 501. HRMS (FAB⁺) *m/z* 454.1410 [(M + H)⁺ calcd for C₂₂H₁₅N₁₁O₂: 454.2013]. Anal. calcd for C₂₂H₁₅N₁₁O₂: C, 56.02; H, 3.38; N, 34.03. Found: C, 55.63; H, 3.33; N, 33.98%.

Compound 2

Compound **2** was prepared by a similar method as described for compound **1**. ¹H NMR (300 MHz, DMSO-d₆) 10.45 (s, 2H, NH), 8.40 (d, ²J(H,H) = 8.7 Hz, 4H; Ar-H), 8.30 (d, ²J(H,H) = 8.4 Hz, 4H; Ar-H), 7.30 (t, ³J(H,H) = 3.9 Hz, 3H; Ar-H). ¹³C NMR (DMSO-d₆) δ = 165, 155, 137, 136, 135, 131, 130, 129, 127, 113 ppm. IR (KBr, cm⁻¹): 3522, 3314, 2963, 2922, 2916, 2915, 2858, 2823, 1959, 1644, 1598, 1524, 1495, 1458, 1318, 1296, 1084, 1036, 1166, 977, 909, 906, 852, 773, 669, 577, 560. HRMS (FAB⁺) *m/z* 452.1458 [(M + H)⁺ calcd for C₂₃H₁₆N₁₀O₂: 452.4313]. Anal. calcd for C₂₃H₁₆N₁₀O₂: C, 58.40; H, 3.26; N, 29.06. Found: C, 57.82; H, 3.23; N, 28.98%.

Acknowledgements

This work was supported by a grant from World Class University (WCU) Program (R32-2008-000-20003-0) and NRF (2010-0018510) supported by Ministry of Education, Science, S. Korea. The work at SKKU was supported by the NRF grant (No. 20100001630) by MEST.

References

- G. O. Lloyd and J. W. Steed, *Nat. Chem.*, 2009, **1**, 437–442.
- R. G. Weiss and P. Terech, *Molecular Gels: Materials with Self-Assembled Fibrillar Networks*, Springer, Dordrecht, 2006.
- Z. Yang, P. L. Ho, G. Liang, K. H. Chow, Q. Wang, Y. Cao, Z. Guo and B. Xu, *J. Am. Chem. Soc.*, 2007, **129**, 266–267.
- S. R. Jadhav, P. K. Vemula, R. Kumar, S. R. Raghavan and G. John, *Angew. Chem., Int. Ed.*, 2010, **49**, 1–5.

- 5 G. John, B. V. Shankar, S. R. Jadhav and P. K. Vemula, *Langmuir*, 2010, **26**, 17843–17851.
- 6 P. K. Vemula, J. Li and G. John, *J. Am. Chem. Soc.*, 2006, **128**, 8932–8938.
- 7 F. Zhao, M. L. Ma and B. Xu, *Chem. Soc. Rev.*, 2009, **38**, 883–891.
- 8 A. Ajayaghosh, V. K. Praveen and C. Vijayakumar, *Chem. Soc. Rev.*, 2008, **37**, 109–122.
- 9 T. H. Kim, M. S. Choi, B. H. Sohn, S. Y. Park, W. S. Lyoo and T. S. Lee, *Chem. Commun.*, 2008, 2364–2366.
- 10 P. Terech and R. G. Weiss, *Chem. Rev.*, 1997, **97**, 3133–3160.
- 11 T. Ishi-I and S. Shinkai, *Top. Curr. Chem.*, 2005, **258**, 119–160.
- 12 L. A. Estroff and A. D. Hamilton, *Chem. Rev.*, 2004, **104**, 1201–1218.
- 13 N. M. Sangeetha and U. Maitra, *Chem. Soc. Rev.*, 2005, **34**, 821–836.
- 14 R. Hirst, B. Escuder, J. F. Miravet and D. K. Smith, *Angew. Chem., Int. Ed.*, 2008, **47**, 8002–8018.
- 15 P. Dastidar, *Chem. Soc. Rev.*, 2008, **37**, 2699–2715.
- 16 M.-O. M. Piepenbrock, G. O. Lloyd, N. Clarke and J. W. Steed, *Chem. Rev.*, 2010, **110**, 1960–2004.
- 17 A. Kishimura, T. Yamashita and T. Aida, *J. Am. Chem. Soc.*, 2005, **127**, 179–183.
- 18 F. Fages, *Angew. Chem., Int. Ed.*, 2006, **45**, 1680–1682.
- 19 S. K. Batabyal, W. L. Leong and J. J. Vittal, *Langmuir*, 2010, **26**, 7464–7468.
- 20 W. L. Leong, A. Y.-Y. Tam, S. K. Batabyal, L. W. Koh, S. Kasapis, V. W.-W. Yam and J. J. Vittal, *Chem. Commun.*, 2008, 3628–3630.
- 21 S. Kawano, N. Fujita and S. Shinkai, *J. Am. Chem. Soc.*, 2004, **126**, 8592–8593.
- 22 K. Tsuchiya, Y. Orihara, Y. Kondo, N. Yoshino, T. Ohkubo, H. Abe and M. J. Sakai, *J. Am. Chem. Soc.*, 2004, **126**, 12282–12283.
- 23 T. Tu, W. Assenmacher, H. Peterlik, R. Weisbarth, M. Nieger and K. H. Dötz, *Angew. Chem., Int. Ed.*, 2007, **46**, 6368–6371.
- 24 B. Xing, M.-F. Choi and B. Xu, *Chem.–Eur. J.*, 2002, **8**, 5028–5032.
- 25 K. Kuroiwa, T. Shibata, A. Takada, N. Nemoto and N. Kimizuka, *J. Am. Chem. Soc.*, 2004, **126**, 2016–2021.
- 26 O. Roubeau, A. Colin, V. Schmitt and R. Clerac, *Angew. Chem., Int. Ed.*, 2004, **43**, 3283–3286.
- 27 M. Shirakawa, N. Fujita, T. Tani, K. Kaneko, M. Ojima, A. Fujii, M. Ozaki and S. Shinkai, *Chem.–Eur. J.*, 2007, **13**, 4155–4162.
- 28 W. Weng, J. B. Beck, A. M. Jamieson and S. J. Rowan, *J. Am. Chem. Soc.*, 2006, **128**, 11663–11672.
- 29 H.-J. Kim, J.-H. Lee and M. Lee, *Angew. Chem., Int. Ed.*, 2005, **44**, 5810–5814.
- 30 S. K. Batabyal, A. M. P. Peedikakkal, S. Ramakrishna, C. H. Sow and J. J. Vittal, *Macromol. Rapid Commun.*, 2009, **15**, 1356–1361.
- 31 T. H. Kim, J. Seo, S. J. Lee, S. S. Lee, J. Kim and J. H. Jung, *Chem. Mater.*, 2007, **19**, 5815–5817.
- 32 F. Camerel, L. Bonardi, M. Schmutz and R. Ziessel, *J. Am. Chem. Soc.*, 2006, **128**, 4548–4549.
- 33 S. Manna, A. Saha and A. K. Nandi, *Chem. Commun.*, 2006, 4285–4287.
- 34 G. D. Paoli, Z. Džolic, F. Rizzo, L. D. Cola, F. Vögtle, W. M. Müller, G. Richardt and M. Žinic, *Adv. Funct. Mater.*, 2007, **17**, 821–828.
- 35 M. Dinca, A. F. Yu and J. R. Long, *J. Am. Chem. Soc.*, 2006, **128**, 8904–8913.
- 36 (a) M. Dinca, A. F. Yu, Y. Liu, C. M. Brown, D. A. Neumann and J. R. Long, *J. Am. Chem. Soc.*, 2006, **128**, 16876–16883; (b) M. Dinca, A. Dailly and J. R. Long, *Chem.–Eur. J.*, 2008, **14**, 10280–10285.
- 37 M. J. Frisch, *Gaussian 03, revision B05*, Gaussian Inc, Pittsburg, PA, 2003.
- 38 T. H. Kim, J. Seo, S. J. Lee, S. S. Lee, J. Kim and J. H. Jung, *Chem. Mater.*, 2007, **19**, 5815–5819.
- 39 B. K. An, D. S. Lee, J. S. Lee, Y. S. Park, H. S. Song and S. Y. Park, *J. Am. Chem. Soc.*, 2004, **126**, 10232–10233.
- 40 A. W. Varnes, R. B. Dodson and E. L. Wehry, *J. Am. Chem. Soc.*, 1972, **94**, 946.
- 41 D. A. Skoog, F. J. Holler and S. R. Crouch, *Principles of Instrumental Analysis*, Thomson, 6th edn, 2007.
- 42 S. Li, L. He, F. Xiong, Y. Li and G. Yang, *J. Phys. Chem. B*, 2004, **108**, 10887–10892.
- 43 S. Kasapis, I. M. Al-Marhoobi, M. Deszynski, J. R. Mitchell and R. Abeysekera, *Biomacromolecules*, 2003, **4**, 1142–1149.